J Gastroenterol
DOI 10.1007/s00535-013-0818-x

ORIGINAL ARTICLE—LIVER, PANCREAS, AND BILIARY TRACT

Histological evaluation of obliterative phlebitis for the diagnosis of autoimmune pancreatitis

Katsuyuki Miyabe · Kenji Notohara · Takahiro Nakazawa · Kazuki Hayashi · Itaru Naitoh · Fumihiro Okumura · Shuya Shimizu · Michihiro Yoshida · Hiroaki Yamashita · Satoru Takahashi · Hirotaka Ohara · Takashi Joh

Received: 11 January 2013 / Accepted: 15 April 2013

Abstract
Background Obliterative phlebitis is a useful pathological finding for the diagnosis of lymphoplasmacytic sclerosing pancreatitis (LPSP), or type 1 autoimmune pancreatitis. The present study evaluated histological findings of obliterative phlebitis, including the significance of adding Elastica van Gieson stain (EVG) in comparison with other pancreatic conditions.
Methods Specimens of LPSP ($n = 18$), chronic pancreatitis (CP; $n = 24$), and pancreatic ductal adenocarcinoma (PDA; $n = 45$) were enrolled. Obliterative venous lesions (OVLs), defined as the presence of inflammatory cells and/or fibrosis inside the tunica adventitia, were counted and compared between hematoxylin and eosin stain (H&E) and EVG. OVLs were classified into three types: OVL-1, lymphoplasmacytic infiltration and fibrosis against a loose textured background; OVL-2, dense fibrosis with minimal or no lymphoplasmacytic infiltration; and OVL-3, densely packed lymphoplasmacytic infiltration without fibrosis. OVL type and OVL size were compared between disease groups.
Results OVL counts in LPSP, CP, and PDA were significantly higher with EVG than with H&E ($p < 0.001$). OVL-1 was most common in LPSP (H&E 92.4 %, EVG 79.8 %), and was identified in almost all cases of LPSP, but was less common in CP and PDA. Maximum diameter and OVL count in 1 cm^2 of OVL-1 were high for LPSP. Maximum diameter of OVL-1 $\geq$150 μm was observed in 17 LPSP, 0 CP, and 1 PDA cases (sensitivity 94.4 %, specificity 98.6 %).
Conclusions Additional EVG is useful for excluding conditions mimicking OVL-1 or detecting OVL in small specimens. The presence of OVL-1 with diameter $\geq$150 μm is highly diagnostic for LPSP.

Keywords Obliterative phlebitis · Autoimmune pancreatitis · IgG4-related disease · Lymphoplasmacytic sclerosing pancreatitis

K. Miyabe · T. Nakazawa (✉) · K. Hayashi · I. Naitoh · F. Okumura · S. Shimizu · M. Yoshida · H. Yamashita · T. Joh
Department of Gastroenterology and Metabolism, Nagoya City University Graduate School of Medical Sciences, 1 Kawasumi, Mizuho-cho, Mizuho-ku, Nagoya 467-8601, Japan
e-mail: tnakazaw@med.nagoya-cu.ac.jp

K. Notohara
Department of Anatomic Pathology, Kurashiki Central Hospital, Kurashiki, Japan

S. Takahashi
Department of Experimental Pathology and Tumor Biology, Nagoya City University Graduate School of Medical Sciences, Nagoya, Japan

H. Ohara
Department of Community-based Medical Education, Nagoya City University Graduate School of Medical Sciences, Nagoya, Japan

Introduction

Autoimmune pancreatitis (AIP) covers a unique group of chronic pancreatitis consisting of two types: type 1, representing lymphoplasmacytic sclerosing pancreatitis (LPSP); and type 2, representing idiopathic duct-centric pancreatitis (IDCP) or AIP with granulocytic epithelial lesion (GEL) [1–3]. Most AIP cases are type 1, and type 2 has been reported infrequently in Japan [4], but may comprise about 20–40 % of AIP cases in the United States and Europe [2, 3, 5].

Since Hamano et al. [6, 7] reported elevated levels of serum immunoglobulin (Ig)G4 (normal <135 mg/dL) and

Published online: 04 May 2013

numerous IgG4-positive plasma cells in tissues affected by AIP, an increased number of IgG4-positive plasma cells, i.e., >10/high-power field (HPF) in most reports, has been adopted as a diagnostic standard for AIP by many pathologists [8, 9]. This finding, however, is not entirely specific for LPSP, as some cases of pancreatic cancer show abundant infiltration of IgG4-positive plasma cells [9–13].

Obliterative phlebitis has also been reported to be present in multifocal fibrosclerosis [14] and LPSP [1, 15]. Because of its characteristic presence in AIP, the existence of obliterative phlebitis is regarded as so important that it has been incorporated into the diagnostic criteria for AIP. However, the methods used to evaluate obliterative phlebitis vary among authors and no consensus has yet been reached regarding which stains are best suited for this evaluation, with some adopting hematoxylin and eosin stain (H&E) alone [3, 16–18] and others applying an additional elastic stain [19–22]. Moreover, little has been discussed regarding characteristic features of obliterative phlebitis for AIP among various pancreatic diseases.

The present study investigated findings of obliterative phlebitis and the significance of additional Elastica van Gieson stain (EVG) for the evaluation of obliterative phlebitis.

Materials and methods

Patients

The files of the Department of Pathology, Nagoya City University Hospital, Kurashiki Central Hospital, and affiliated hospitals between 1976 and 2009 were searched for pancreas resections for which the final diagnosis was chronic pancreatitis (CP). All cases underwent operation with a clinical diagnosis of pancreatic cancer. Open biopsy specimens larger than 1 cm^2 were also included in this study.

All H&E-stained slides were reviewed by two authors (K.M. and K.N.) blinded to clinical information, identifying 18 cases with LPSP and 24 with CP. All LPSP cases showed full-blown histological features other than obliterative phlebitis, such as: abundant (≥50 cells/HPF) IgG4-positive plasma cells; marked lymphoplasmacytic infiltration with fibrosis and without granulocytic infiltration; periductal inflammation; and storiform fibrosis. CP cases consisted of both alcoholic and idiopathic CP, and were diagnosed on the basis of the Zurich classification [23], such as history of excessive alcohol intake, calcification in the pancreas, or moderate to marked ductal lesions as described in the Cambridge classification [24] Patients who had consumed >80 g/dL of alcohol for some years were diagnosed with excessive alcohol intake [23]. Cases without other causes of CP, such as nutritional, hereditary, cystic fibrosis, hypercalcemia, or trauma, were classified as idiopathic. The pathology of CP is characterized by perilobular fibrosis and acinar destruction with acute and chronic inflammatory cells [25]. Forty-five resected specimens of pancreatic ductal adenocarcinoma (PDA) were also included in this study.

The study protocol was approved by the review board of Nagoya City University Graduate School of Medical Sciences (Approval No. 284).

Histology and Immunohistochemistry

Resected specimens were fixed in formalin and embedded in paraffin. For each case, the representative tissue block showing the most marked fibrosis and inflammatory cell infiltration was selected. Serial 3-μm thick sections were made from paraffin-embedded tissue blocks, then stained with H&E, EVG, and immunostained with mouse anti-human IgG4 monoclonal antibody (MC011, dilution 1:100; The Binding Site, Birmingham, UK) using a DISCOVERY HX automated immunostainer (Ventana Medical Systems, Tucson, AZ, USA).

All slides were reviewed in a blinded manner by two independent authors (K.M., a gastroenterologist with training in pancreatic pathology while in graduate school; and K.N., a specialist in pathology certified by the Japanese Society of Pathology) who were blinded to clinical information. When assessments differed between the two observers, a consensus decision was reached using a double-headed microscope. Slides were observed under light microscopy (ECLIPSE 80i; Nikon, Tokyo, Japan) using a 10× objective lens and 10× ocular lens, corresponding to a field diameter of 2.2 mm for slides.

Definition of venous lesions

In order to take venous lesions with scarce inflammation into consideration, the term "obliterative venous lesion" (OVL) was adopted in this study, rather than "obliterative phlebitis". OVL was defined as the presence of inflammatory cells and/or fibrosis inside the venous tunica adventitia under a low-power view in which the entire circumference of the venous wall could be confirmed with H&E or EVG. OVLs with invading adenocarcinoma inside or predominant neutrophilic infiltration were excluded from this investigation.

OVL count

We evaluated total OVL counts on both stained slides in each case and compared them between stains in LPSP, CP, and PDA.

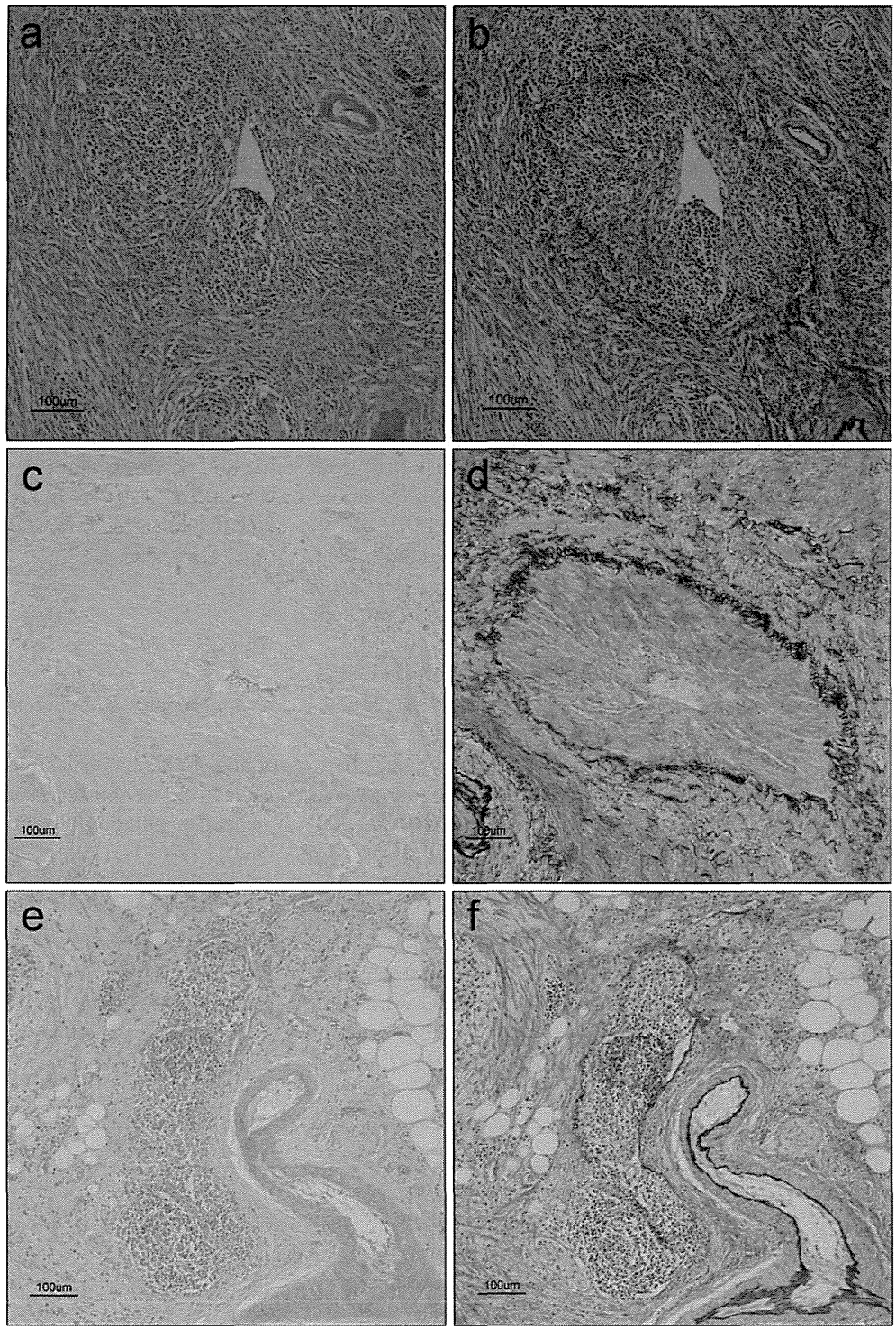

Fig. 1 Pictures of obliterative venous lesions (OVLs). OVL-1 with **a** H&E and **b** EVG, showing OVL filled with lymphoplasmacytic infiltration and fibrosis against a loose-textured background. OVL-2 with **c** H&E and **d** EVG, showing OVL filled with dense fibrosis with minimal or no lymphoplasmacytic infiltration. OVL-3 with **e** H&E and **f** EVG, OVL filled with densely packed lymphoplasmacytic infiltration without fibrosis. ×100

OVL classification

We classified OVLs into three types based on the extent of inflammation and fibrosis, as follows (Fig. 1): OVL-1, OVL filled with lymphoplasmacytic infiltration and fibrosis against a loose-textured background; OVL-2, OVL filled with dense fibrosis with minimal or no lymphoplasmacytic infiltration; and OVL-3, OVL filled with densely packed lymphoplasmacytic infiltration without fibrosis.

These OVL types were identified on HE or EVG slides. Percentages of OVL count for each OVL type in a disease group were compared between LPSP and CP/PDA with both stains.

OVL prevalences, OVL count in 1 cm^2, and OVL size

In addition to OVL count, we also evaluated prevalences of each OVL type (i.e., each OVL percentage among a disease group) and count per 1 cm^2 in inflamed areas. Specimen areas on slides with marked fibrosis and inflammatory cells were measured using IPAP software (version 3.0.1; Sumika Technoservice Corporation, Osaka, Japan). OVL count divided by specimen area with marked fibrosis and inflammatory cells in each case was calculated as the OVL count in 1 cm^2.

For investigating OVL size in each OVL type, we measured OVL diameter and compared mean, minimum, and maximum diameters. OVLs were scanned as pictures in a low-power field with ACT-1 software (version 2.6.3; Nikon, Tokyo, Japan). OVL diameter was measured with these scanned pictures using the Scale tool of Adobe Photoshop CS4 extended software (version 11.0.2; Adobe Systems, Berkeley, CA, USA). Mean, minimum, and maximum diameters were calculated only among cases with each OVL type, because cases without any OVL type precluded precise calculation.

OVL prevalences, OVL counts in 1 cm^2, and OVL sizes (mean, minimum, and maximum diameters) were compared between LPSP and CP/PDA.

We also analyzed receiver-operating characteristic (ROC) curves for different pathologies, to determine sensitivity, specificity and accuracy compared to other diseases for the optimal cut-off value.

Statistical analysis

Statistical analyses were performed using non-parametric tests. OVL differences between H&E and EVG were compared using the Mann–Whitney U test, Pearson's χ^2, or Fisher's exact test. Differences in sex, OVL-1, -2, and -3 counts, and the numbers of cases with each OVL type between LPSP and CP/PDA were compared using Pearson's χ^2 or Fisher's exact test with Bonferroni correction. Differences in age, OVL-1, -2, and -3 percentages in individual cases, OVL counts in 1 cm^2, and OVL diameters between LPSP and CP/PDA were determined using Dunnett's multiple comparison test if the Kruskal–Wallis test between three disease groups showed significant results. For ROC curves, the best cut-off values were chosen according to the highest diagnostic accuracy determined using the Youden index: sensitivity − (1 − specificity) [26, 27]. ROC curves that correlated with areas under the curve (AUCs) were compared by nonparametric comparisons [28].

All tests were two-sided. Values of $p < 0.05$ without Bonferroni correction and $p < 0.025$ with Bonferroni correction (two comparisons between three groups) were considered statistically significant. Statistical analysis was performed using JMP software (version 8.0.2; SAS Institute, Cary, NC, USA).

Results

Demographics and clinical presentation

Clinical characteristics for the present series of LPSP, CP, and PDA were not greatly different from those in the general population (Table 1) [29–35].

Comparison of OVL counts between H&E and EVG

In every case, total OVL counts were higher with EVG than with H&E in LPSP (median 24.5 vs. 8.0), CP (4.0 vs. 0), and PDA (7.0 vs. 2.0) (Fig. 2a; $p < 0.001$ each). In fact, many OVLs were found to be missed using H&E alone (Fig. 3a, b).

Table 1 Clinical data of the cases used in this study

	LPSP ($n = 18$)	CP ($n = 24$)	PDA ($n = 45$)
Age (mean, range)	66 (54–79)	48.5 (14–67)*	67 (32–82)
Sex (male/female)	17/1	23/1	30/15†
Sign and symptoms			
Obstructive jaundice	10	0	15
Abdominal pain or back pain	6	19	17
Excessive alcohol intake	2 (NA, 3 cases)	18	3 (NA, 1 case)
Radiographic findings			
Mass forming	18	7	45
Calcification in the pancreas	0	16	1
Surgical procedure			
PD or PpPD	13	7	27
DP	4	16	17
Open biopsy	1	1	1

Patients who had consumed >80 g/day of alcohol for some years were considered to have excessive alcohol intake

PD pancreaticoduodenectomy, *PpPD* pylorus-preserving pancreaticoduodenectomy, *DP* distal pancreatectomy and splenectomy, *NA* not available

* $p < 0.0001$, † $p = 0.0221$

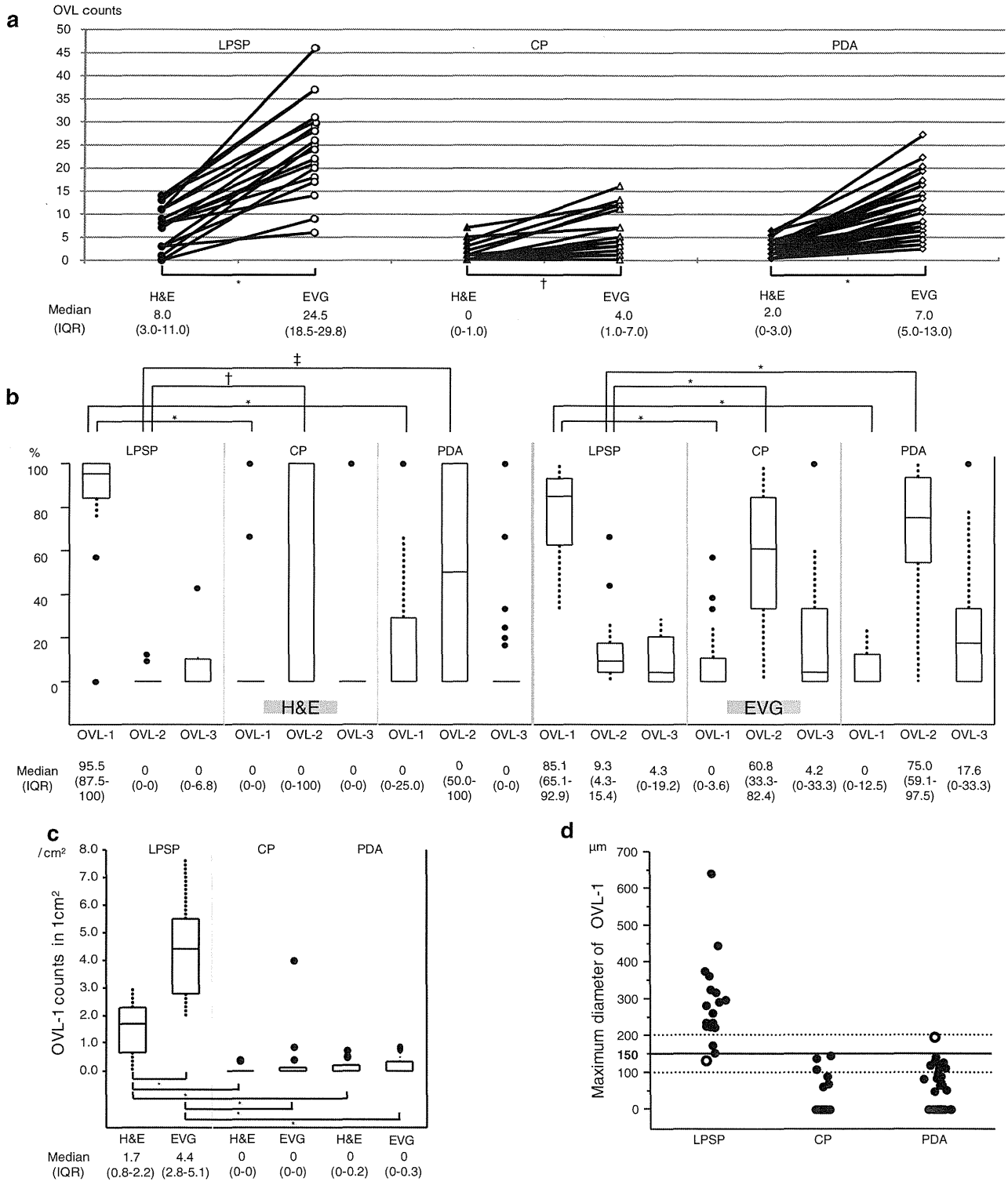

Fig. 2 **a** OVL counts in a case with H&E and EVG stains. *IQR* interquartile range; $*p < 0.0001$; $^{\dagger}p = 0.0005$. **b** *Box-and-whisker* plots of OVL percentages in individual cases. $*p < 0.0001$; $^{\dagger}p = 0.0003$; $^{\ddagger}p = 0.0214$. **c** *Box-and-whisker* plots of OVL-1 count in 1 cm^2 in a case. $*p < 0.0001$; *n.s.* not significant. **d** *Dot* plot of the maximum diameter of OVL-1 in each case. In **b** and **c**, *boxes* represent the IQR of data, *lines across boxes* indicate median values, *hash marks* depict the nearest value within 1.5 × the IQR, and *black dots* indicate outliers. In **d**, a *solid line* indicates a cut-off value of 150 μm and *white circles* indicate inapplicable cases to this value. Comparisons between H&E and EVG were performed using the Mann–Whitney *U* test and Dunnett's test was used for comparisons between LPSP and CP/PDA if the Kruskal–Wallis test for comparisons of three disease groups yielded significant results. The remaining comparisons between LPSP and CP/PDA or between H&E and EVG had no significance. The *p* values are results of Dunnett's test, Pearson's χ^2 test or Fisher's extract test, and the Mann–Whitney *U* test

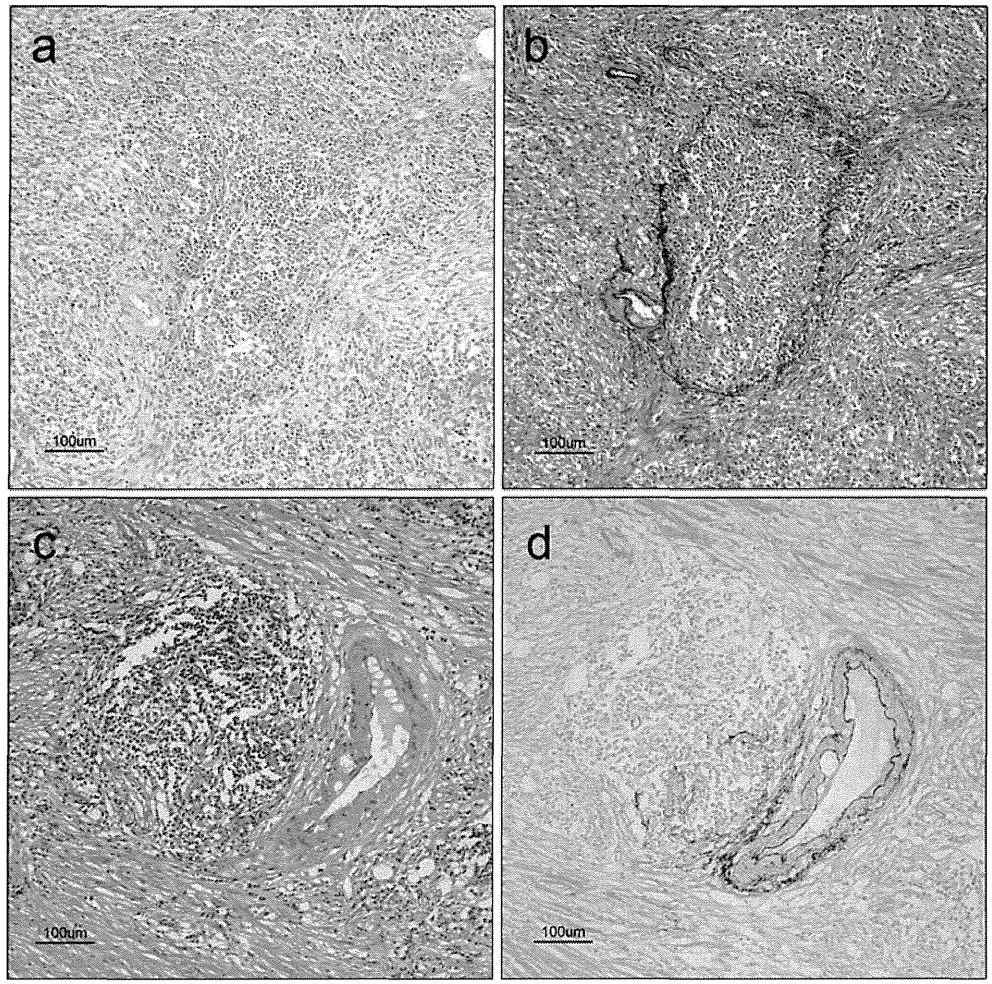

Fig. 3 *Above* OVL that could be overlooked. This lesion with **a** H&E was hard to identify without **b** EVG. *Below* a lymphoid aggregate that could easily be mistaken for OVL. Lymphoid aggregates adjacent to an artery could easily be misinterpreted as OVLs with only **c** H&E. However, in this field, **d** EVG reveals that only a small portion represents true OVL. ×100

Comparison of OVL counts after classification

OVL counts for each OVL type in LPSP, CP, and PDA groups are summarized in Table 2. OVL-1 was more common in the LPSP group (92.4 % with H&E) than in the CP and PDA groups ($p < 0.0001$ for H&E and EVG), whereas OVL-2 was more common in the CP and PDA groups (85.2 and 69.1 % with H&E, respectively) than in the LPSP group ($p < 0.0001$ for H&E and EVG).

Percentages of OVL-1 in LPSP and PDA groups were significantly higher with H&E alone than with the aid of EVG (LPSP 92.4 vs. 79.8 %, $p = 0.0008$; PDA 17.3 vs. 7.2 %, $p = 0.0035$) and the percentage of OVL-2 in the LPSP group was significantly higher with EVG than with H&E (11.1 vs. 2.3 %, respectively; $p = 0.0009$). OVL-1 in the CP group did not differ significantly between stains, although several lesions of OVL-1 were observed in both CP and PDA (Fig. 4).

When we counted OVLs in individual cases, percentages of OVL-1 in a case were larger for LPSP (median 95.5 % with H&E and 85.1 % with EVG) than for CP (0 % with H&E and EVG) or PDA (0 % with H&E and EVG) with both stains (Fig. 2b; all comparisons, $p < 0.0001$).

Features of OVL-1 were the same as the features of surrounding tissue. Some lymphoid aggregates adjacent to arteries could be easily misinterpreted as OVL-1 on H&E-stained slides. In this context, EVG was helpful for detecting true OVLs (Fig. 3c, d).

Comparison of OVL prevalences, OVL count in 1 cm^2, and OVL size

OVL-1 was identified in almost all cases in the LPSP group (16/18 with H&E, 18/18 with EVG), but was less common in the CP (2/24 with H&E, 6/24 with EVG) and PDA (12/45 with H&E, 18/45 with EVG) groups (Table 3). In all disease groups, the number of cases with OVL-1 did not differ significantly by adding EVG for evaluation, whereas the numbers of cases with OVL-2 and OVL-3 were larger with the aid of EVG than with H&E alone, with the exception of OVL-3 in the LPSP (all comparisons, $p < 0.05$).

Total OVL counts in 1 cm^2 were significantly larger in the LPSP group (median, 1.9 with H&E, 5.3 with EVG)

Table 2 OVL counts in LPSP, CP, and PDA groups

	LPSP (H&E, 132; EVG, 440 OVLs)		CP (H&E, 27; EVG, 120 OVLs)		PDA (H&E, 81; EVG, 416 OVLs)		*p* value LPSP vs CP	*p* value LPSP vs PDA
OVL-1								
H&E	122 (92.4%)	p=0.0008	3 (11.1%)	n.s.	14 (17.3%)	p = 0.0035	<0.0001	<0.0001
EVG	351 (79.8%)		14 (11.7%)		30 (7.2%)		<0.0001	<0.0001
OVL-2								
H&E	3 (2.3%)	p=0.0009	23 (85.2%)	n.s.	56 (69.1%)	n.s.	<0.0001	<0.0001
EVG	49 (11.1%)		85 (70.8%)		300 (72.1%)		<0.0001	<0.0001
OVL-3								
H&E	7(5.3%)	n.s.	1 (3.7%)	n.s.	11 (13.6%)	n.s.	n.s.	n.s.
EVG	40(9.1%)		21 (17.5%)		86(20.7%)		0.0071	<0.0001

OVL counts (percentages among each disease group); *p* values are results of Pearson's χ^2 test or Fisher's extract test. Bonferroni correction was applied to compare between LPSP and CP/PDA

n.s. not significant

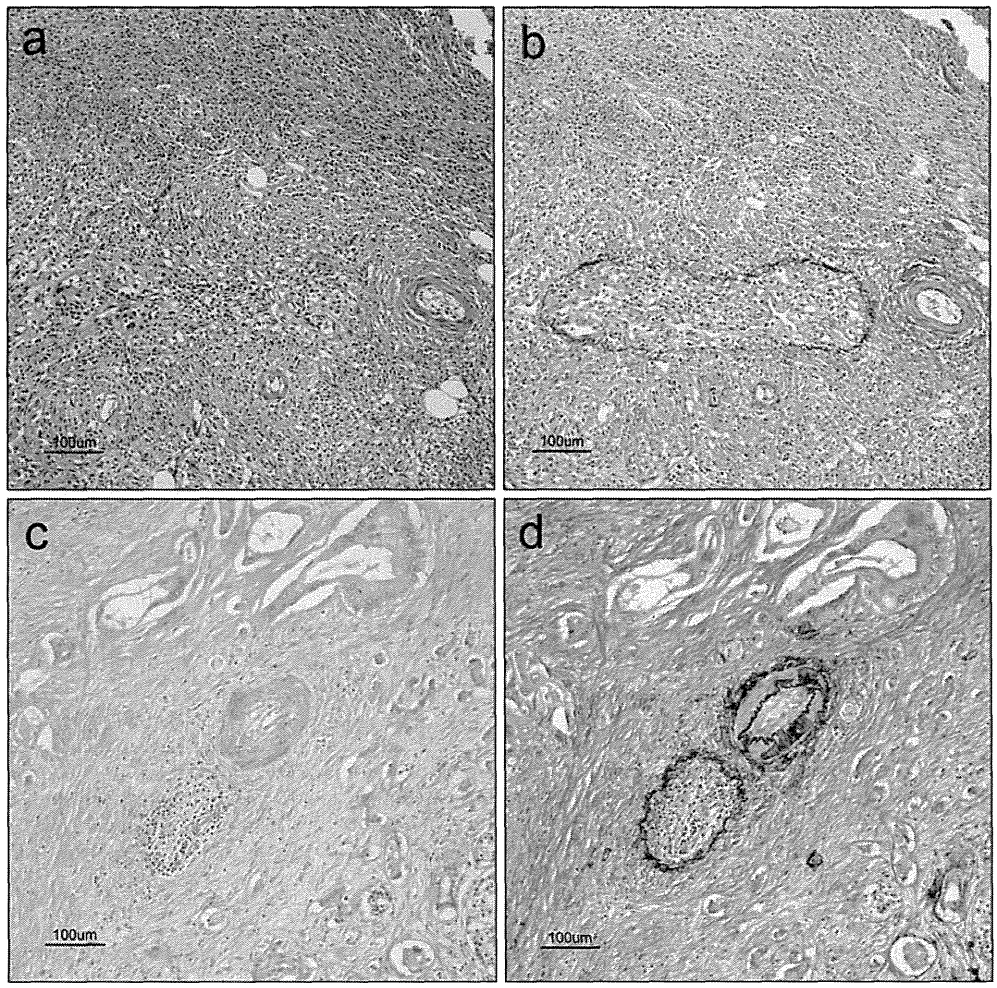

Fig. 4 OVL-1 found in CP and PDA. OVL-1 in a CP case (alcoholic CP, 48-year-old man) with **a** H&E and **b** EVG. OVL-1 in a PDA case (71-year-old woman) with **c** H&E and **d** EVG (×100)

than in CP (0 with H&E, 1.0 with EVG) or PDA (0.4 with H&E, 2.3 with EVG) groups with both stains (all comparisons, $p < 0.0001$). In the LPSP group, OVL-1 counts in 1 cm^2 were significantly larger with EVG than with H&E ($p < 0.0001$); however, in the CP and PDA groups, no significant differences in counts were seen between stains (Fig. 2c).

Mean, minimum, and maximum diameters for each OVL type are shown in Table 4 (cases without OVLs were excluded in this result).

Table 3 The number of cases and prevalence with each OVL type

	LPSP ($N = 18$)		CP ($N = 24$)		PDA ($N = 45$)		p value	
							LPSP vs CP	LPSP vs PDA
Any OVL								
H&E	16 (88.9%)	n.s.	11 (45.8%)	$p = 0.0145$	32 (71.1%)	$p < 0.0001$	0.0081	n.s.
EVG	18 (100%)		20 (83.3%)		45 (100%)		n.s.	n.s.
OVL-1								
H&E	16 (88.9%)	n.s.	2 (8.3%)	n.s.	12 (26.7%)	n.s.	<0.0001	<0.0001
EVG	18 (100%)		6 (25.0%)		18 (40%)		<0.0001	<0.0001
OVL-2								
H&E	3 (16.7%)	$p<0.0001$	9 (37.5%)	$p = 0.0077$	25 (55.6%)	$p < 0.0001$	n.s.	0.0057
EVG	16 (88.9%)		19 (79.2%)		44 (97.8%)		n.s.	n.s.
OVL-3								
H&E	5 (27.8%)	n.s.	1 (4.2%)	$p = 0.0007$	9 (20.0%)	$p < 0.0001$	0.0059	n.s.
EVG	11 (61.1%)		12 (50.0%)		32 (71.1%)		n.s.	n.s.

The number of cases (prevalences, i.e. percentages among a disease group); p values are results of Pearson's χ^2 test or Fisher's extract test. Bonferroni correction was applied to compare between LPSP and CP/PDA

n.s. not significant

Table 4 Mean, minimum, and maximum diameters with each OVL type

	LPSP	CP	PDA	p value	
				vs CP	vs PDA
Mean diameter (μm)					
All OVLs[a]	124 (95.2–139.8)	90.9 (65.3–120.7)	90.3 (72.6–107.9)	n.s	
OVL-1[b]	131.1 (112.2–151.6)	83.1 (70.8–104.7)	79.2 (65–89.4)	0.0285	0.0006
OVL-2[c]	81.4 (68.1–100.2)	98.5 (68.1–137.8)	89.3 (66.7–112.2)	n.s	
OVL-3[d]	106.4 (62–124.4)	63.5 (52.3–97.5)	87.4 (76–100.2)	n.s	
Minimum diameter (μm)					
All OVLs[a]	41.0 (33.1–47.8)	44.1 (33.2–61.8)	41.0 (31.3–47.0)	n.s	
OVL-1[b]	51.7 (45.1–57.7)	64.4 (54.7–84.5)	64.5 (50.8–83.6)	n.s	
OVL-2[c]	52.2 (41.1–70.2)	51.2 (34.6–95.6)	41.5 (32.0–51.4)	n.s	
OVL-3[d]	54.8 (42.5–67.7)	57.8 (52.3–63.7)	65.4 (45.4–80.1)	n.s	
Maximum diameter (μm)					
All OVLs[a]	285.4 (224.5–322.6)	137.4 (107.1–196.1)	155.7 (126.2–233.9)	0.0154	0.0013
OVL-1[b]	270.6 (224.5–322.6)	98.5 (74.1–129.8)	96.7 (72.1–118.4)	<0.0001	<0.0001
OVL-2[c]	113.2 (88.5–142.1)	142.4 (116.6–204)	148.9 (94.5–234.4)	n.s	
OVL-3[d]	133.2 (77.1–222.3)	64.5 (52.3–120)	119.8 (85.7–138.5)	n.s	

Median (interquartile range); cases without OVLs were excluded in this table. Dunnett's test was used for comparisons between LPSP and CP/PDA if the Kruskal–Wallis test for comparisons of the three disease groups yielded significant results. p values are results of Dunnett's test. Cases without OVLs were excluded. Calculated cases were as follows: [a] 18 LPSP, 20 CP, and 45 PDA cases; [b] 18 LPSP, 6 CP, and 17 PDA cases; [c] 6 LPSP, 19 CP, and 44 PDA cases; [d] 10 LPSP, 12 CP, and 32 PDA cases

n.s. not significant

No significant differences in minimum diameter of any OVL type were apparent between LPSP and CP/PDA. Maximum diameter of total OVLs was significantly larger for LPSP than for CP ($p = 0.0154$) or PDA ($p = 0.0013$). Mean and maximum diameters of OVL-1 were significantly larger for LPSP than for CP (mean, $p = 0.0285$; maximum, $p < 0.0001$) or PDA (mean, $p = 0.0006$; maximum, $p < 0.0001$).

Cut-off values for the diagnosis of LPSP

We performed ROC analysis for mean diameter, maximum diameter, and OVL count in 1 cm^2 for total OVLs and OVL-1 (Table 5). Optimal cut-off values (sensitivity/specificity, AUC) for mean diameter, maximum diameter, and count in 1 cm^2 of OVL-1 for differentiating LPSP from CP and PDA were 79.8 μm (100 %/82.1 %, 0.9493),

Table 5 Outcomes analyzed by receiver-operating characteristic (ROC) curves for each parameter of all OVLs and OVL-1

	Cut-off value	Sensitivity (%)	Specificity (%)	Accuracy (%)	AUC (95 % CI)	*p* value
All OVLs						
Mean diameter (μm)	111.0	72.2	78.3	75.2	0.7665 (0.6315–0.8628)	n.s.
Maximum diameter (μm)	220.6	83.3	76.8	80.1	0.8225 (0.7056–0.8996)	0.0006
OVL count in 1 cm^2						
H&E	1.3	72.2	94.2	83.2	0.8527 (0.6779–0.9409)	<0.0001
EVG	3.6	94.4	82.6	88.5	0.9275 (0.8539–0.9655)	<0.0001
OVL-1						
Mean diameter (μm)	79.8	100.0	82.1	91.1	0.9493 (0.8850–0.9785)	<0.0001
Maximum diameter (μm)					0.9952 (0.9727–0.9992)	<0.0001
Best cut-off value	131.5	100.0	94.2	97.1		
Proposed cut-off value	150.0	94.4	98.6	96.5		
OVL count in 1 cm^2						
H&E	0.4	88.9	94.2	91.5	0.9283 (0.7708–0.9804)	<0.0001
EVG	1.9	100.0	98.6	99.3	0.9936 (0.9523–0.9992)	<0.0001

Cut-off values were chosen with the highest diagnostic accuracy determined using the Youden index: sensitivity − (1 − specificity). Areas under the curve (AUCs) that correlated with ROC curves were compared by nonparametric comparison

n.s. not significant, *95 % CI* 95 % confidence interval

131.5 μm (100 %/94.2 %, 0.9952), and 0.4/cm^2 (88.9 %/94.2 %, 0.9283) with H&E and 1.9/cm^2 (100 %/98.6 %, 0.9936) with EVG, respectively. All optimal cut-off values for each parameter in OVL-1 were superior to those in all OVLs. These results indicated that maximum diameter and OVL count in 1 cm^2 of OVL-1 were very precise for the diagnosis of LPSP. The AUC of OVL-1 was significantly better for maximum diameter than for mean diameter ($p = 0.0174$) and showed no significant differences between mean diameter and OVL count in 1 cm^2, and maximum diameter and OVL count in 1 cm^2.

As shown in Fig. 2d, 18 LPSP, 3 CP, and 5 PDA cases showed maximum diameter of OVL-1 ≥100 μm (sensitivity 100 %, specificity 88.4 %), while 17 LPSP, 0 CP, and 1 PDA cases showed maximum diameter ≥150 μm (sensitivity 94.4 %, specificity 98.6 %), and 15 LPSP, 0 CP, and 0 PDA cases showed maximum diameter ≥200 μm (sensitivity 83.3 %, specificity 100 %).

When we added all OVLs together, OVL-1 with diameter ≥150 μm was found in 34.5 % (OVLs, 121/351), 0 % (0/14), and 6.7 % (2/30) in the LPSP, CP, and PDA groups, respectively.

Discussion

The concept of obliterative phlebitis appears to have been first described for two patients with Riedel's thyroiditis in 1931 [36], and was later confirmed by another group [37]. Obliterative phlebitis has also been reported in a group of pathologies that are now recognized as IgG4-related diseases [38], such as orbital pseudotumour [39], retroperitoneal fibrosis [7, 40], AIP [3–5, 9, 10], sclerosing cholangitis [30, 41], inflammatory pseudotumour of the liver [42], and lungs [43], but may be inconspicuous or absent in organs such as the lymph nodes [51], lungs [43], minor salivary glands, and lachrymal glands [49, 52]. Obliterative phlebitis is so unique and pathognomonic that it has been included in the histological diagnostic criteria for AIP such as the International Consensus Diagnostic Criteria, the HISORt Criteria, the Japanese Diagnostic Criteria, the Korean Criteria, and the Asian Criteria [13, 44–48]. Histologically, it is characterized by obliteration of small veins following lymphoplasmacytic infiltration and fibrosis. This finding often reveals nodular inflammation adjacent to a small artery, because arteries and veins are anatomically adjacent in the pancreas. According to recently published consensus statement on the pathology of IgG4-related disease, obliterative phlebitis is defined as the obliteration of venous channels by a dense lymphoplasmacytic infiltrate and is additionally explained as showing lymphocytes and plasma cells both within the walls of venous channels and within the lumen [49]. However, recognition of obliterative phlebitis is often difficult using H&E alone, and the usefulness of additional elastic stain has not yet been evaluated sufficiently, although some articles have mentioned that stains for elastic fibers such as Movat pentachrome or EVG are helpful for identifying the lesion [21, 50].

The present study used the term OVL instead of obliterative phlebitis to take various inflammatory venous occlusions into account. Thus, OVL probably shows a

broader spectrum of venous lesions than originally intended. Even so, OVL was significantly more common for LPSP than for CP or PDA in this study. This finding may indicate that OVL-1 could be more readily detected from small biopsy specimens. In fact, Bang et al. detected 5 of 19 AIP patients (26 %) using ultrasonography-guided core biopsy [12]. Chari et al. reported that 7 of 16 (44 %) core biopsies showed the full spectrum of diagnostic changes for LPSP, including obliterative phlebitis [45]. Given the importance of the histological identification of obstructive phlebitis for the biopsy diagnosis of LPSP, accurate evaluation of venous lesions seems crucial.

We compared histological features of OVL among LPSP, CP, and PDA. A similar classification of obliterative phlebitis was reported previously by Meijer et al. [37] for Riedel's thyroiditis. In fact, our histological classification of OVL resembles theirs, with OVL-1, -2 and -3 corresponding to their occlusive stage (obliteration with granulation tissue), sclerosing stage (replacement of obliterated lumens by collagen) and infiltrative stage (lymphoplasmacytic infiltration in veins), respectively. However, we speculate that the histological variety of OVL may not necessarily be attributable to differences in the stage of inflammation.

A typical example of this problem remains in OVL-2, which in our classification is considered to represent the scarring of various lesions, and both organized thrombi and old obliterative phlebitis could take this form. Given that vessel walls are commonly damaged in pancreatitis by the activated lipase, OVL-2 could conceivably also be the result of venous damage and secondary obstruction by organized thrombi. In fact, OVL-2 identified in CP and PDA is likely caused by organized thrombi. In LPSP, distinguishing whether each OVL-2 lesion is due to organized thrombus or organization of obliterative phlebitis is difficult. While OVL-2 may be a form of true obliterative phlebitis, a safer statement would be to say that OVL-2 is nonspecific, and should not be regarded as obliterative phlebitis for diagnostic purposes.

We also suspect that OVL-3 truly corresponds to inflammatory obliteration of veins. In our experience, this finding is common at the waning or edge of veins, suggesting that OVL-3 forms primarily at tangential sectioning of veins with inflammatory cells in the walls. The present data suggest that OVL-3 is nonspecific for LPSP and commonly observed even in CP and PDA.

This study found that OVL-1 was more specific to LPSP. Although several lesions of OVL-1 were observed in CP and PDA, percentages were significantly higher in LPSP than in CP and PDA for both group counts and individual case counts. OVL-1 was identified in almost all cases of LPSP (16/18 with H&E, 18/18 with EVG), but was less common in CP and PDA. These findings indicate that OVL-1, rather than OVL-2 or -3, should be recognized as diagnostic for LPSP and we suggest that OVL-2 and OVL-3 be excluded from the diagnostic criteria for obliterative phlebitis. The correlation between the three types of OVLs and pathogenesis of AIP and the applicability of OVL-1 for other organs of IgG4-related disease were not investigated in this study.

Elastica van Gieson stain could depict a greater number of OVL than H&E. This is concordant with the findings of a previous study that described Movat pentachrome stain as 100 % sensitive and 99 % specific for identifying obliterative phlebitis [21]. However, in the present study, the significance of EVG differed depending on the type of OVL. That is, EVG was not particularly useful for identifying OVL-1, whereas OVL-2 was almost impossible to identify without the help of EVG. Therefore, considering the significance of OVL-1 for the diagnosis of LPSP, EVG does not appear essential for identifying obliterative phlebitis.

Nevertheless, EVG remains rather useful in some situations. Storiform fibrosis, another characteristic feature of LPSP, may form a nodular inflammatory lesion, and can thus be difficult to distinguish from obliterative phlebitis if such a focus is seen adjacent to an artery. EVG did depict otherwise unclear OVLs, and may be necessary when making a diagnosis with biopsy tissue. Even so, we must stress that the histological features of obliterated veins should be always reevaluated by identification and examination of the lesion on H&E-stained slides.

We also elucidated that the maximum diameter of OVL-1 was larger for LPSP than for CP or PDA. To clarify the usefulness of maximum diameter of OVL-1, we performed ROC analysis of parameters. While the optimal cut-off value of maximum diameter was 131.5 μm (sensitivity 100 %, specificity 94.2 %), we would propose OVL-1 $\geq$ 150 μm in maximum diameter on surgical specimen (sensitivity 94.4 %, specificity 98.6 %) as a clinically useful value without sacrificing diagnostic accuracy. Although the field diameter of light microscopy is fixed at manufacture, OVL-1 occupying more than one-third of the diameter in a 400× field is diagnostic of LPSP.

Lymphoplasmacytic sclerosing pancreatitis should be diagnosed using three histopathological features: dense lymphoplasmacytic infiltrate; storiform fibrosis; and obliterative phlebitis. A diagnosis should not be made using only one of these features [49]. IgG4 immunostaining is also an essential test for the pathological diagnosis of IgG4-related disease. However, a large number of conditions other than IgG4-related disease can be associated with increased numbers of IgG4-positive plasma cells in tissue and LPSP should also not be diagnosed based solely on findings from IgG4-positive plasma cells [49]. In these conditions, the criteria of OVL-1 $\geq$150 μm could be useful

for improving the diagnostic accuracy of LPSP on surgical specimens.

Although we were not been able to conduct a study using fine needle aspiration (FNA) samples because of our limited experience with FNA specimens, we surmise that OVL-1 is unlikely to be seen in large venules with a FNA specimen, because application of the criteria of OVL-1 $\geq$150 μm depends on the sample size and specimens gathered by EUS-FNA are too small to detect large veins. A separate diameter criterion for FNA specimens thus appears warranted, whereas dense OVL-1 counts in 1 cm^2 in LPSP also indicate that OVL-1 would be diagnostic and even identifiable in biopsy samples.

The key limitation in this study was that specimens of LPSP, CP, and PDA were assembled retrospectively. This was an unfortunate necessity, because LPSP is an uncommon disease and few cases of LPSP haven been operated on recently because of improvements in LPSP diagnosis. Moreover, we were unable to investigate OVL in type 2 AIP, as few cases of type 2 AIP are encountered in Japan. Further investigation to clarify these issues is necessary.

In conclusion, we believe that the presence of OVL-1 is diagnostic for LPSP. In particular, OVL-1 with diameter $\geq$150 μm is highly diagnostic for LPSP by itself. Additional EVG, despite offering limited significance, can improve the identification of OVL and be useful in some situations, such as identifying no OVL with H&E. These criteria will improve the precision of detecting obliterative phlebitis and should prove useful in diagnosing patients with LPSP.

Acknowledgments We are indebted to Seizoh Nagaya, Department of Clinical Pathology, Nagoya City University Graduate School of Medical Sciences; Yukimi Itoh, Department of Gastroenterology and Metabolism, Nagoya City University Graduate School of Medical Sciences; Hitoshi Sano, Department of Gastroenterology, Gifu Prefectural Tajimi Hospital; and Hiroki Takada, Department of Gastroenterology, Kasugai Municipal Hospital for providing the tissue specimens, clinical information, and technical assistance with histological analysis. Katsuyuki Miyabe received a Travel Grant from Toyoaki Scholarship Foundation; Kenji Notohara, Takahiro Nakazawa, and Hirotaka Ohara received a Grand-in-Aid for "Research for Intractable Disease" Program from the Ministry of Health, Labor and Welfare of Japan; Takahiro Nakazawa and Itaru Naitoh received a Grants-in-Aid for Scientific Research from the Ministry of Culture and Science of Japan (23591015 to Takahiro Nakazawa and 23790803 to Itaru Naitoh).

Conflict of interest All the authors declared neither competing interests nor funding disclosures pertaining to this article.

References

1. Kawaguchi K, Koike M, Tsuruta K, Okamoto A, Tabata I, Fujita N. Lymphoplasmacytic sclerosing pancreatitis with cholangitis: a variant of primary sclerosing cholangitis extensively involving pancreas. Hum Pathol. 1991;22(4):387–95.
2. Notohara K, Burgart LJ, Yadav D, Chari S, Smyrk TC. Idiopathic chronic pancreatitis with periductal lymphoplasmacytic infiltration: clinicopathologic features of 35 cases. Am J Surg Pathol. 2003;27(8):1119–27.
3. Zamboni G, Luttges J, Capelli P, Frulloni L, Cavallini G, Pederzoli P, et al. Histopathological features of diagnostic and clinical relevance in autoimmune pancreatitis: a study on 53 resection specimens and 9 biopsy specimens. Virchows Arch. 2004;445(6):552–63.
4. Chari ST, Kloeppel G, Zhang L, Notohara K, Lerch MM, Shimosegawa T. Histopathologic and clinical subtypes of autoimmune pancreatitis: the Honolulu consensus document. Pancreas. 2010;39(5):549–54.
5. Park DH, Kim MH, Chari ST. Recent advances in autoimmune pancreatitis. Gut. 2009;58(12):1680–9.
6. Hamano H, Kawa S, Horiuchi A, Unno H, Furuya N, Akamatsu T, et al. High serum IgG4 concentrations in patients with sclerosing pancreatitis. N Engl J Med. 2001;344(10):732–8.
7. Hamano H, Kawa S, Ochi Y, Unno H, Shiba N, Wajiki M, et al. Hydronephrosis associated with retroperitoneal fibrosis and sclerosing pancreatitis. Lancet. 2002;359(9315):1403–4.
8. Deheragoda MG, Church NI, Rodriguez-Justo M, Munson P, Sandanayake N, Seward EW, et al. The use of immunoglobulin g4 immunostaining in diagnosing pancreatic and extrapancreatic involvement in autoimmune pancreatitis. Clin Gastroenterol Hepatol. 2007;5(10):1229–34.
9. Zhang L, Notohara K, Levy MJ, Chari ST, Smyrk TC. IgG4-positive plasma cell infiltration in the diagnosis of autoimmune pancreatitis. Mod Pathol. 2007;20(1):23–8.
10. Deshpande V, Chicano S, Finkelberg D, Selig MK, Mino-Kenudson M, Brugge WR, et al. Autoimmune pancreatitis: a systemic immune complex mediated disease. Am J Surg Pathol. 2006;30(12):1537–45.
11. Ghazale A, Chari ST, Smyrk TC, Levy MJ, Topazian MD, Takahashi N, et al. Value of serum IgG4 in the diagnosis of autoimmune pancreatitis and in distinguishing it from pancreatic cancer. Am J Gastroenterol. 2007;102(8):1646–53.
12. Bang SJ, Kim MH, Kim do H, Lee TY, Kwon S, Oh HC, et al. Is pancreatic core biopsy sufficient to diagnose autoimmune chronic pancreatitis? Pancreas. 2008;36(1):84–9.
13. Otsuki M, Chung JB, Okazaki K, Kim MH, Kamisawa T, Kawa S, et al. Asian diagnostic criteria for autoimmune pancreatitis: consensus of the Japan-Korea Symposium on Autoimmune Pancreatitis. J Gastroenterol. 2008;43(6):403–8.
14. Meyer S, Hausman R. Occlusive phlebitis in multifocal fibrosclerosis. Am J Clin Pathol. 1976;65(3):274–83.
15. Wreesmann V, van Eijck CH, Naus DC, van Velthuysen ML, Jeekel J, Mooi WJ. Inflammatory pseudotumour (inflammatory myofibroblastic tumour) of the pancreas: a report of six cases associated with obliterative phlebitis. Histopathology. 2001; 38(2):105–10.
16. Yadav D, Notahara K, Smyrk TC, Clain JE, Pearson RK, Farnell MB, et al. Idiopathic tumefactive chronic pancreatitis: clinical profile, histology, and natural history after resection. Clin Gastroenterol Hepatol. 2003;1(2):129–35.
17. Levy MJ, Wiersema MJ, Chari ST. Chronic pancreatitis: focal pancreatitis or cancer? Is there a role for FNA/biopsy? Autoimmune pancreatitis. Endoscopy. 2006;38 Suppl 1:S30–5.
18. Chen TS, Montgomery EA. Are tumefactive lesions classified as sclerosing mesenteritis a subset of IgG4-related sclerosing disorders? J Clin Pathol. 2008;61(10):1093–7.
19. Suda K, Takase M, Fukumura Y, Ogura K, Ueda A, Matsuda T, et al. Histopathologic characteristics of autoimmune pancreatitis based on comparison with chronic pancreatitis. Pancreas. 2005; 30(4):355–8.

20. Ito H, Kaizaki Y, Noda Y, Fujii S, Yamamoto S. IgG4-related inflammatory abdominal aortic aneurysm associated with autoimmune pancreatitis. Pathol Int. 2008;58(7):421–6.
21. Chu KE, Papouchado BG, Lane Z, Bronner MP. The role of Movat pentachrome stain and immunoglobulin G4 immunostaining in the diagnosis of autoimmune pancreatitis. Mod Pathol. 2009;22(3):351–8.
22. Kamisawa T, Okazaki K, Kawa S, Shimosegawa T, Tanaka M. Japanese consensus guidelines for management of autoimmune pancreatitis: III. Treatment and prognosis of AIP. J Gastroenterol. 2010;45(5):471–7.
23. Ammann RW. A clinically based classification system for alcoholic chronic pancreatitis: summary of an international workshop on chronic pancreatitis. Pancreas. 1997;14(3):215–21.
24. Sarner M, Cotton PB. Classification of pancreatitis. Gut. 1984; 25(7):756–9.
25. Suda K, Shiotsu H, Nakamura T, Akai J. Pancreatic fibrosis in patients with chronic alcohol abuse: correlation with alcoholic pancreatitis. Am J Gastroenterol. 1994;89(11):2060–2.
26. Fluss R, Faraggi D, Reiser B. Estimation of the Youden Index and its associated cutoff point. Biom J. 2005;47(4):458–72.
27. Youden WJ. Index for rating diagnostic tests. Cancer. 1950;3(1): 32–5.
28. DeLong ER, DeLong DM, Clarke-Pearson DL. Comparing the areas under two or more correlated receiver operating characteristic curves: a nonparametric approach. Biometrics. 1988; 44(3):837–45.
29. Raina A, Yadav D, Krasinskas AM, McGrath KM, Khalid A, Sanders M, et al. Evaluation and management of autoimmune pancreatitis: experience at a large US center. Am J Gastroenterol. 2009;104(9):2295–306.
30. Ghazale A, Chari ST, Zhang L, Smyrk TC, Takahashi N, Levy MJ, et al. Immunoglobulin G4-associated cholangitis: clinical profile and response to therapy. Gastroenterology. 2008;134(3): 706–15.
31. Frulloni L, Scattolini C, Falconi M, Zamboni G, Capelli P, Manfredi R, et al. Autoimmune pancreatitis: differences between the focal and diffuse forms in 87 patients. Am J Gastroenterol. 2009;104(9):2288–94.
32. Nishimori I, Tamakoshi A, Otsuki M. Prevalence of autoimmune pancreatitis in Japan from a nationwide survey in 2002. J Gastroenterol. 2007;42 Suppl 18:6–8.
33. Otsuki M. Chronic pancreatitis in Japan: epidemiology, prognosis, diagnostic criteria, and future problems. J Gastroenterol. 2003;38(4):315–26.
34. Garg PK, Tandon RK. Survey on chronic pancreatitis in the Asia-Pacific region. J Gastroenterol Hepatol. 2004;19(9):998–1004.
35. Cress RD, Yin D, Clarke L, Bold R, Holly EA. Survival among patients with adenocarcinoma of the pancreas: a population-based study (United States). Cancer Causes Control. 2006;17(4):403–9.
36. Roulet F. Über eigenartige Gefäßbefunde bei chronischer Thyreoiditis (eisenharte Struma Riedel). Virchows Arch. 1931; 280(3):640–8.
37. Meijer S, Hausman R. Occlusive phlebitis, a diagnostic feature in Riedel's thyroiditis. Virchows Arch A Pathol Anat Histol. 1978;377(4):339–49.
38. Stone JH, Zen Y, Deshpande V. IgG4-related disease. N Engl J Med. 2012;366(6):539–51.
39. Mombaerts I, Goldschmeding R, Schlingemann RO, Koornneef L. What is orbital pseudotumor? Surv Ophthalmol. 1996;41(1): 66–78.
40. Mitchinson MJ. The pathology of idiopathic retroperitoneal fibrosis. J Clin Pathol. 1970;23(8):681–9.
41. Nakazawa T, Ando T, Hayashi K, Naitoh I, Ohara H, Joh T. Diagnostic procedures for IgG4-related sclerosing cholangitis. J Hepatobiliary Pancreat Sci. 2011;18(2):127–36.
42. Zen Y, Fujii T, Sato Y, Masuda S, Nakanuma Y. Pathological classification of hepatic inflammatory pseudotumor with respect to IgG4-related disease. Mod Pathol. 2007;20(8):884–94.
43. Zen Y, Inoue D, Kitao A, Onodera M, Abo H, Miyayama S, et al. IgG4-related lung and pleural disease: a clinicopathologic study of 21 cases. Am J Surg Pathol. 2009;33(12):1886–93.
44. Shimosegawa T, Chari ST, Frulloni L, Kamisawa T, Kawa S, Mino-Kenudson M, et al. International consensus diagnostic criteria for autoimmune pancreatitis: guidelines of the International Association of Pancreatology. Pancreas. 2011;40(3):352–8.
45. Chari ST, Smyrk TC, Levy MJ, Topazian MD, Takahashi N, Zhang L, et al. Diagnosis of autoimmune pancreatitis: the Mayo Clinic experience. Clin Gastroenterol Hepatol. 2006;4(8):1010–6 (quiz 934).
46. Chari ST, Takahashi N, Levy MJ, Smyrk TC, Clain JE, Pearson RK, et al. A diagnostic strategy to distinguish autoimmune pancreatitis from pancreatic cancer. Clin Gastroenterol Hepatol. 2009;7(10):1097–103.
47. Okazaki K, Kawa S, Kamisawa T, Naruse S, Tanaka S, Nishimori I, et al. Clinical diagnostic criteria of autoimmune pancreatitis: revised proposal. J Gastroenterol. 2006;41(7):626–31.
48. Kim KP, Kim MH, Kim JC, Lee SS, Seo DW, Lee SK. Diagnostic criteria for autoimmune chronic pancreatitis revisited. World J Gastroenterol. 2006;12(16):2487–96.
49. Deshpande V, Zen Y, Chan JK, Yi EE, Sato Y, Yoshino T, et al. Consensus statement on the pathology of IgG4-related disease. Mod Pathol. 2012;25(9):1181–92.
50. Smyrk TC. Pathological features of IgG4-related sclerosing disease. Curr Opin Rheumatol. 2011;23(1):74–9.
51. Cheuk W, Yuen HK, Chu SY, et al. Lymphadenopathy of IgG4-related sclerosing disease. Am J Surg Pathol. 2008;32:671–81.
52. Cheuk W, Yuen HK, Chan JK. Chronic sclerosing dacryoadenitis: part of the spectrum of IgG4-related Sclerosing disease? Am J Surg Pathol. 2007;31:643–5.

Japan College of Rheumatology
MODERN RHEUMATOLOGY

http://informahealthcare.com/mor
ISSN 1439-7595 (print), 1439-7609 (online)

Mod Rheumatol, 2013; Early Online: 1–6

DOI: 10.3109/14397595.2013.844307

informa
healthcare

ORIGINAL ARTICLE

Clinicopathological features of IgG4-related disease complicated with orbital involvement

Chihiro Hagiya[1], Hiroto Tsuboi[1], Masahiro Yokosawa[1], Shinya Hagiwara[1], Tomoya Hirota[1], Chinatsu Takai[1], Hiromitsu Asashima[1], Haruka Miki[1], Naoto Umeda[1], Masanobu Horikoshi[1], Yuya Kondo[1], Makoto Sugihara[1], Hiroshi Ogishima[1], Takeshi Suzuki[1], Takahiro Hiraoka[2], Yuichi Kaji[2], Isao Matsumoto[1], Tetsuro Oshika[2], and Takayuki Sumida[1]

[1]*Departments of Internal Medicine, Faculty of Medicine, University of Tsukuba, Tsukuba, Japan and* [2]*Department of Opthalmology, Faculty of Medicine, University of Tsukuba, Tsukuba, Japan*

Abstract

Objective. IgG4-related disease (IgG4-RD) is characterized by IgG4-positive plasmacytic infiltration and fibrosis in various organs. Orbital involvement in IgG4-RD includes lacrimal glands, extra-ocular muscles, trigeminal nerve and other parts of the orbit. Immunohistochemical staining is used to diagnose IgG4-RD in patients with orbital inflammation. The purpose of this retrospective study was to clarify the clinicopathological features of IgG4-RD complicated with orbital involvement.

Methods. We examined the clinical features, pathological findings and response to treatment in nine patients with IgG4-RD who underwent orbital tissue biopsy between April 2010 and August 2012 at the University of Tsukuba Hospital.

Results. Among the nine patients, eight had dacryoadenitis, one had infraorbital nerve swelling, and another one had IgG4-related orbital inflammation. Involvement of other organs was identified in all patients, including involvement of the salivary glands, lymph nodes, lung, kidney and para-aorta. In all patients, biopsy samples from orbital tissues showed lymphoplasmacytic infiltration and fibrosis, and IgG4-positive/IgG-positive plasmacyte ratio of > 40%. All patients were treated with prednisolone (0.6 mg/kg/day) and responded well in early phase, although relapse was noted in two patients following tapering of prednisolone, evident by swelling of lacrimal glands.

Conclusion. Patients with IgG4-RD complicated with orbital involvement often present with involvement of other organs. The histopathological findings of orbital tissue match the characteristic features of IgG4-RD. Corticosteroid is effective for orbital and systemic involvement in IgG4-RD.

Keywords

IgG4-related disease, Orbital involvement

History

Received 16 April 2013
Accepted 30 May 2013
Published online 18 October 2013

Introduction

IgG4-related disease (IgG4-RD) is a new disease entity characterized by elevated serum IgG4 concentration, swelling of organs associated with IgG4-positive plasmacytic infiltration and fibrosis [1, 2]. IgG4-RD might involve various organs throughout the body, such as the central nervous system, lacrimal gland, salivary gland, thyroid, lung, liver, pancreas, bile duct, gastrointestinal tract, kidney, prostate, retroperitoneum, arteries, lymph nodes, skin and breast [1, 2].

Mikulicz's disease (MD) is characterized by symmetric swelling of lacrimal glands and salivary glands and currently considered a major subgroup of IgG4-RD [1]. The pathological findings of lacrimal and salivary glands in MD are similar to the characteristic features of IgG4-RD, such as IgG4-positive plasmacytic infiltration and fibrosis [1]. Several studies have recently reported the involvement of many intra-orbital tissues in IgG4-RD, including extra-ocular muscles, trigeminal nerve and other portions of the orbit as well as lacrimal glands [3–5]. Moreover, it is reported that IgG4-specific immunohistochemical staining can be used to clarify IgG4-positive plasmacytic infiltration in patients with orbital pseudotumor of unknown etiology [6]. Thus, it is possible to diagnose orbital pseudotumor as IgG4-RD using immunohistochemistry. Because Stone et al. proposed to use "IgG4-related orbital inflammation" instead of "orbital pseudotumor" occurring in the context of IgG4-RD in 2012 [5], we use this term in this manuscript.

In addition, recent reports showed that patients with IgG4-RD complicated with orbital involvement often have systemic IgG4-related lesions rather than intra-orbital tissues [3, 4]. These findings suggest that orbital lesions of IgG4-RD, including MD, can be regarded as organ involvement in systemic lesions of IgG4-RD.

The purpose of this study was to clarify the clinical and pathological features and response to treatment of patients with IgG4-RD and orbital involvement.

Correspondence to: Prof. Takayuki Sumida, Department of Internal Medicine, Faculty of Medicine, University of Tsukuba, 1-1-1 Tennodai, Tsukuba-city, Ibaraki 305-8575, Japan. Tel: +81-29-853-3221. Fax: +81-29-853-3222. E-mail: tsumida@md.tsukuba.ac.jp

Patients and methods

We examined nine patients with definite IgG4-RD who underwent orbital tissue biopsy between April 2010 and August 2012 at the University of Tsukuba Hospital (Ibaraki, Japan). Orbital tissues included lacrimal glands and orbital inflammation. All nine patients were diagnosed as definite IgG4-RD based on the 2011 diagnostic criteria of IgG4-RD proposed by the All Japan IgG4 Team [7], which include the presence of all of the following three items: (1) characteristic diffuse/localized swelling or masses in single or multiple organs on clinical examination, (2) high serum IgG4 concentrations (> 135 mg/dl) detected on blood tests and (3) marked lymphocyte and plasmacyte infiltration and fibrosis, plus ratio of infiltrating IgG4-positive/IgG-positive plasma cells of >40%, with >10 IgG4-positive plasma cells/high-power field on histopathological examination. In this retrospective study, we also scanned the medical records for clinical background, orbital involvement, involvement of other organs, laboratory data, pathological findings, response to treatment and prognosis. Approval for this study was obtained from the local ethics committee and a signed informed consent was obtained from each subject.

Results

Clinical background

Table 1 shows the clinical background of the nine patients (age: 40–60 years, five males, four females). Although all nine patients had orbital involvement, two (Patients 3 and 6) had extra-orbital symptoms but not orbital symptoms, at the time of admission. Only one patient complained of dry eye. Four patients had a history of allergy (Patient 1; rhinitis, Patient 4; asthma, Patient 6; cough variant asthma, Patient 7; asthma).

Orbital and systemic involvement

Table 2 lists the organs involved. Of the nine patients, eight had lacrimal gland involvements, and one of them also had infraorbital nerve swelling, and another had IgG4-related orbital inflammation. Macroscopically, his left eye was bulged. Magnetic resonance imaging (MRI) revealed that this orbital inflammation was the area of low signal intensity both on T1-weighted imaging (T1WI) and on T2-weighted imaging (T2WI). Because he had bronchial asthma, we could not perform contrast study. The mass of orbital inflammation was inner extraocular muscle cones of left eye, which compressed optic nerve on the inside. The mass grew extraconus and spread into ethmoid sinus (Figure 1). Neurosurgeons operated the biopsy of this mass by endoscopic endonasal approach.

All eight patients with lacrimal gland involvement also had salivary gland involvement and were diagnosed as MD. Involvement of other organs was also observed in all nine patients, including the lymph nodes in all nine patients, thickening of the broncho-vascular bundle in two patients, autoimmune pancreatitis in one patient, kidney and urinary tract involvements such as thickening of pyelic and urethral wall, hilar mass, and interstitial nephritis in five patients and para-artery in four patients.

Table 1. Clinical background of nine patients.

Case	Age	Gender	Main complaint	History of allergy
1	47	F	Swelling of eyelid and dry eye	Rhinitis
2	58	F	Neck tumor and eyelid tumor	None
3	47	M	Lumbago	None
4	59	M	Swelling of eye and double vision	Asthma
5	55	M	Swelling of eyelid	None
6	64	F	Swelling of submaxillary and parotid areas	Cough variant asthma
7	78	F	Swelling and pain of eyelid	Asthma
8	66	M	Lumbago and swelling of eyelid	None
9	63	M	Swelling and redness of eyelid	None

M: male, F: female

Laboratory data

Table 3 shows the results of laboratory tests conducted before treatment. Eight patients had high-serum IgG levels and all nine patients had high-serum IgG4 levels (≧135 mg/dl). However, none had renal dysfunction, high-serum amylase, or abnormal liver function tests. Soluble interleukin-2 receptor (sIL-2R) was increased in eight patients, whereas complement titer was decreased in two patients. IgE levels were high in seven patients, and anti-nuclear antibodies (ANA) by immunofluorescence assay were positive in two patients (40 times, homogeneous pattern in Patient 6, and 1,280 times, centromere pattern in Patient 9). Anti SS-A antibody by Ouchterlony assay was positive in only one patient (Patient 1), whereas anti-SS-B antibody was negative in all nine patients.

Table 2. Orbital and other organ involvements.

	Orbital involvement*								
Case	LG	Others	SG	LN	Lung	Pancreas	Kidney and urinary tract	Para-artery	Others
1	○	—	○	Intraparotid LN, Cer	—	—	—	—	—
2	○	Infraorbital nerve	○	Pel	—	—	Interstitial nephritis	PA and aorta	—
3	○	—	○	Cer, Par	—	—	Thickening of the pyelic and urethral wall	—	—
4	—	Inner muscle cone inflammation	—	Cer, Med, Hil, Pel	—	—	—	Aorta	Obturator nerve
5	○	—	○	Cer, Med, Hil	—	—	—	Subclavian and vertebral A	—
6	○	—	○	Cer, Med, Hil, Par	○¶	—	Soft tissue mass of renal hilus, Thickening of the pyelic wall	—	—
7	○	—	○	Cer, Med, Hil	—	—	—	—	—
8	○	—	○	Ing	—	—	Soft tissue mass of renal hilus	Aorta	Para-vertebral mass, prostate
9	○	—	○	Intraparotid LN, Cer, Axi, Med, Hil, Mes, Pel	○¶	Autoimmune pancreatitis	Thickening of the pyelic and urethral wall	—	Para-vertebral mass

LG: lacrimal glands, SG: salivary glands, LN: lymph nodes (Cer: cervical LN, Axi: axillary LN, Med: mediastinal LN, Hil: hilar LN, Par: Paraartery LN, Mes: mesenteric LN, Pel: pelvic LN, Ing: inguinal LN), PA: pulmonary artery, A: arteries, ○: positive, —: negative

*Orbital involvement: lacrimal glands, nerves and inner muscle cone inflammation.

¶Thickened broncho-vascular bundle

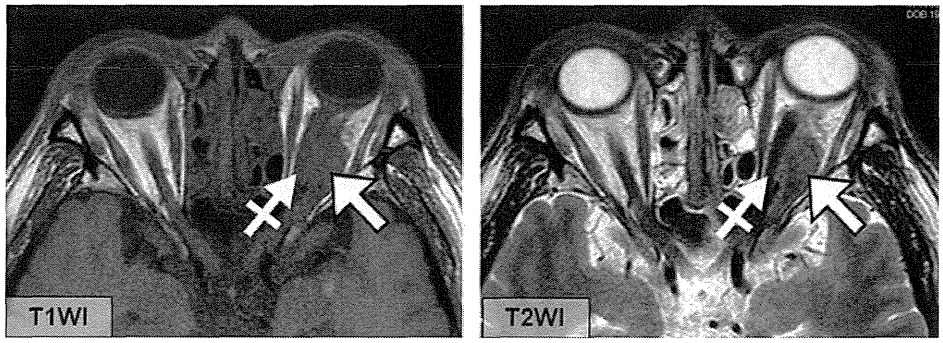

Figure 1. MRI findings of orbital inflammation in Patient 4. This IgG4-related orbital inflammation (*arrows*) was the area of low signal intensity both on T1WI and on T2WI. The mass of orbital inflammation was inner extraocular muscle cones of left eye, which compressed optic nerve on the inside (The cross arrows point out left optic nerve).

Table 3. Results of laboratory tests conducted before treatment.

Case	IgG (mg/dL) (870–1700)	IgG4 (mg/dL) (4.8–105)	Cre (mg/dL) (M: 0.61–1.04 F: 0.47–0.79)	AMY (mg/dL) (40–126)	AST (IU/L) (8–38)	ALT (IU/L) (4–44)	sIL-2R (U/mL) (124–466)	CH50 (U/mL) (31.6–57.6)	IgE (mg/dL) (0–170)	ANA (times)	SS-A/B (times)
1	1363	304	0.51	50	17	16	296	49.1	238	<40	1/−
2	1899	773	0.71	109	16	17	750	34.8	96	<40	−/−
3	1965	478	0.7	62	20	14	1740	<10.0	156	<40	−/−
4	3131	1590	0.83	113	36	26	1080	50.8	1289	<40	−/−
5	2766	1090	0.61	61	17	17	746	40.4	504	<40	−/−
6	3232	1710	0.62	139	25	11	748	56.6	437	40 (homo)	−/−
7	3376	1990	0.95	65	33	19	840	59.8	2015	<40	−/−
8	2236	951	0.77	74	26	18	559	54.1	105	<40	−/−
9	7696	4570	0.77	38	15	7	2790	<10.0	1016	1280 (cent)	−/−
Mean± SD	3074 ± 1864.7	1495 ±1284.0	0.72 ± 0.131	79 ± 33.6	23 ± 7.7	16 ± 5.3	1061 ± 760.8	ND	651 ± 660.5	ND	ND

Homo: homogeneous pattern, Cent: centromere pattern, sIL-2R: soluble interleukin-2 receptor, M: male, F: female, ND: not determined.

Table 4. Pathological findings of orbital tissues and other organs.

	Intra-orbit				Extra-orbit			
Case	Tissue	Lymphoplasmacytic infiltration	Fibrosis	IgG4/IgG	Tissue	Lymphoplasmacytic infiltration	Fibrosis	IgG4/IgG
1	Lacrimal gland	○	△ (slight)	62%		Not performed		
2	Lacrimal gland	○	○	80%	Labial salivary gland	○	○	3%
3	Lacrimal gland	○	○	60%	Thickening of the pyelic and urethral wall	○	○	ND
4	Inner muscle cone inflammation	○	○	95%	Mucosa of nasal cavity	○	○	ND
5	Lacrimal gland	○	○	80%	Labial salivary gland	○	○	80%
6	Lacrimal gland	○	○	95%	Labial salivary gland	○	—	ND
7	Lacrimal gland	○	○	80%		Not performed		
8	Lacrimal gland	○	○	80%	Labial salivary gland	○	○	75%
					Inguinal lymph node	—	—	—
9	Lacrimal gland	○	○	85%	Labial salivary gland	○	○	80%

IgG4/IgG: ratio of IgG4-positive plasmacytes/IgG-positive plasmacytes, ○: positive, —: negative, ND: not determined.

Pathological findings in orbital tissues and other organs

Table 4 summarizes the pathological findings in orbital tissues and other organs. All biopsy samples isolated from orbital tissues showed lymphoplasmacytic infiltration and fibrosis (slight fibrosis in lacrimal glands was noted in one patient, mild to moderate fibrosis in other patients). Immunohistochemistry showed that ratio of IgG4-positive plasmacytes/IgG-positive plasmacytes was > 40% in all orbital tissues (Figures 2 and 3). These findings indicate that the pathological changes in orbital tissues of IgG4-RD were in agreement with the characteristic features of IgG4-RD.

Seven of nine patients underwent biopsy of extra-orbital tissues, including labial salivary glands (LSGs) in five patients, pyelic wall, mucosa of the nasal cavity and right inguinal lymph node in one patient, respectively. The pathological findings in all five LSGs were lymphoplasmacytic infiltration and fibrosis, and three patients showed infiltration of many IgG4-positive plasmacytes. Although examination of the pyelic wall and nasal cavity also showed lymphoplasmacytic infiltration, IgG4-specific immunohistochemical studies were not performed. One lymph node showed neither lymphoplasmacytic infiltration nor fibrosis, and IgG4-positive plasmacytes were not detected by immunohistochemical staining. Moreover, the pathological findings in this lymph node did not correspond with other diseases such as lymphoma, Castleman's disease, or other connective tissue diseases.

Response to treatment and prognosis

Table 5 summarizes the response to treatment and prognosis. All nine patients were treated with corticosteroids (oral prednisolone). The initial dosage was 0.6 mg/kg/day, which was then tapered by 10% biweekly in all nine patients. The therapeutic effect was

Mod Rheumatol, 2013; Early Online: 1–6

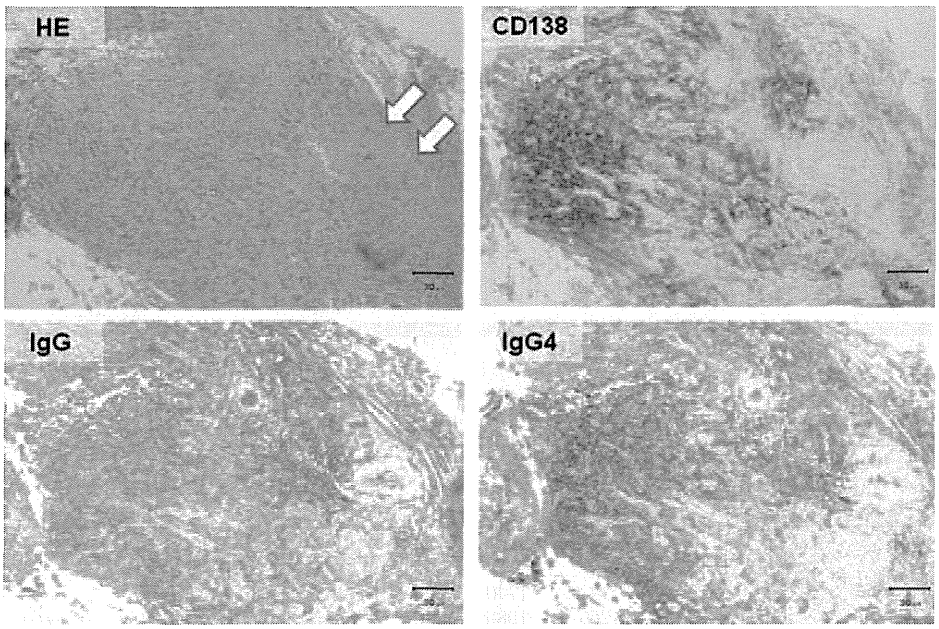

Figure 2. Pathological findings of orbital inflammation in Patient 4. Note the lymphoplasmacytic infiltration and mild fibrosis (arrows), and the presence of IgG4-positive plasmacytes (original magnification, X40). HE, hematoxylin–eosin staining; CD138, immunohistochemical staining for CD138; IgG, immunohistochemical staining for IgG; IgG4, immunohistochemical staining for IgG4.

excellent in the early phase in each patient; not only the orbital involvement but also the involvement of the other organs improved in all patients. With tapering of the corticosteroids, two patients (Patients 1 and 3) experienced relapse (2/9 cases, 22.2%) with swelling of lacrimal glands. Re-elevation of serum IgG4 level in Patient 1 showed an increase in IgG4 level to 133 mg/dl at 23 months after initiation of treatment compared with the minimum value of 93.0 mg/dl recorded at 19 months. The dose of prednisolone at the time of relapse was 9 mg/day in Patient 1 and 10 mg/day in Patient 3.

Discussion

In this study, we described the clinical and pathological features and response to treatment in nine patients with IgG4-RD complicated with orbital involvement. The orbital involvement varied among the patients, from involvement of the lacrimal glands, infraorbital nerve and IgG4-related orbital inflammation. In addition to such lesions, previous studies also described the involvement of intra-orbital muscles and lacrimal sacs in IgG4-RD [3, 5, 6, 8]. Among the orbital complications in IgG4-RD, the lacrimal glands were the most affected in this study and the study of Takahira et al. [8].

Importantly, extra-orbital involvement was noted in every patient, which also varied from one patient to another. Involvement of the salivary glands and lymph nodes was the most common, followed by pelvic mass and para-artery involvements, while autoimmune pancreatitis was detected only in one patient in the present study. The results are in agreement with those of a previous report which found the salivary glands and lymph nodes to be the most common extra-orbital lesions in 16 patients with IgG4-related orbital inflammation [8]. Therefore, it is important to examine

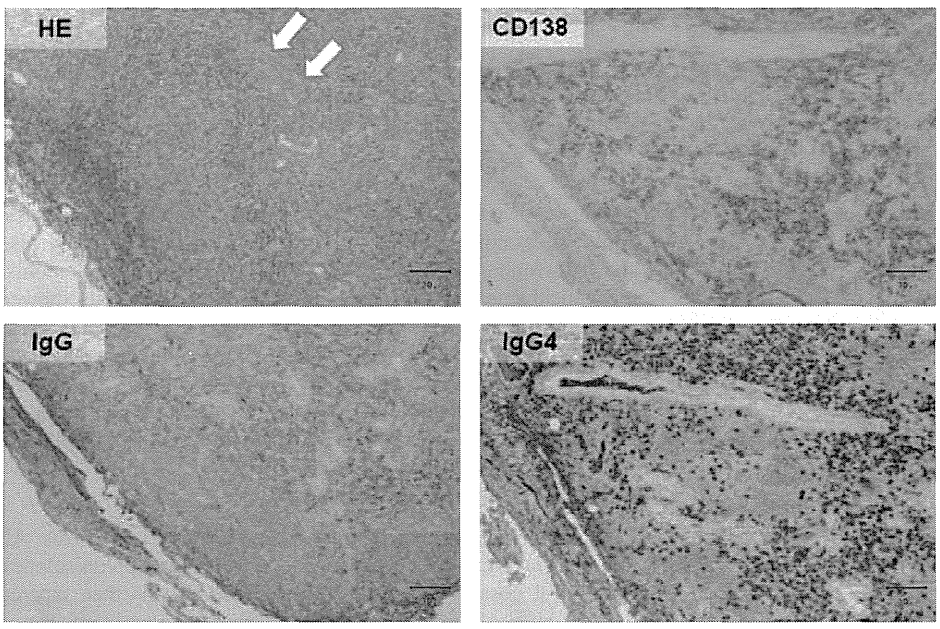

Figure 3. Pathological findings of lacrimal gland in Patient 6. Note the lymphoplasmacytic infiltration and mild fibrosis (*arrows*), and the presence of IgG4-positive plasmacytes (original magnification, X40). HE, CD138, IgG and IgG4; same as in Figure 2.

Table 5. Response to treatment.

Case	Initial PSL dose (mg/day)	Response to treatment: Orbital involvement*	Other organ involvement		IgG4 (mg/dL): Baseline	1-month later	Last test	Follow-up period (month)	PSL dose at last follow-up (mg/day)	Relapse
1	30	Improved	SG, LN	Improved	304	162	133	23	9	swelling of LG
2	30	Improved	SG, LN, interstitial nephritis para-artery	Improved	773	311	60.3	10	10	—
3	30	Improved	LN, thickening of the pyelic and urethral wall	Improved	478	167	83.9	9	10	swelling of LG
			SG	No changed						
4	40	Improved	LN, para-artery, obturator nerve	Improved	1590	407	203	9	10	—
5	40	Improved	SG, para-artery	Improved	1090	615	ND	9	10	—
			LN	No changed						
6	30	Improved	SG, LN, lung, pelvic mass, thickening of the pyelic wall	Improved	1710	535	185	8	10	—
7	30	Improved	SG, LN	Improved	1990	ND	ND	4	15	—
8	35	Improved	SG, LN, pelvic mass, para-artery, PVM, prostate	Improved	951	765	ND	3	20	—
9	35	Improved	SG, LN, lung, pancreas, thickening of the pyelic and urethral wall, PVM	Improved	4570	896	466	2	20	—

PVM: para-vertebral mass, PSL: prednisolone, LG: lacrimal glands, SG: salivary glands, LN: lymph nodes.
*Orbital involvement included lacrimal glands, nerves and inner muscle cone inflammation.

the entire body by imaging studies such as computed tomography (CT) with contrast enhancement to detect systemic complications in IgG4-RD, even in patients with clinical symptoms limited to orbital involvement.

With regard to the pathological features, marked lymphoplasmacytic infiltration, fibrosis and a high IgG4+/IgG+ plasma cell ratio (>40%) were identified in each orbital tissue biopsy. Lacrimal gland biopsy was performed in the present study after local anesthesia and minimum skin dissection. Sufficient volume of lacrimal gland tissue was obtained by this procedure for pathological diagnosis, with minimal invasion compared to other organs. In comparison, obtaining biopsies from the salivary glands, submandibular and parotid glands is more invasive than lacrimal glands biopsy. Although labial salivary gland biopsy is conducted with local anesthesia, this procedure is associated with false-negative results. Interestingly, one patient out of five patients (20%) in this study who underwent labial salivary gland biopsy had only few IgG4-positive plasmacytes (IgG4-positive/IgG-positive plasmacytes ratio of 3%) (Table 4). Hermet et al. [9] also reported negative immunostaining with anti-IgG4 antibody of labial salivary gland biopsy in one patient out of five IgG4-RD patients with dry mouth. Considered together, the results suggest a high diagnostic value for lacrimal gland biopsy. Biopsy and histopathological examination, especially that of lacrimal glands, should be performed in patients with orbital involvement.

We confirmed that the response to treatment with corticosteroids was very well in the early phase with reductions in orbital tissue swelling and serum IgG4 levels. Based on the current experience, care should be taken to avoid relapse in the later phase when the dose of prednisolone is tapered to around 10 mg/day. The relapse ratio in this study (2/9 cases, 22.2%) was similar to that reported in a recent study by Khosroshahi and Stone [10]. Further analysis is needed to determine the best approach for treatment of relapse in such patients and maintenance of remission. In this regard, previous studies suggested re-increasing the dose of corticosteroids [11], or the use of azathioprine [11–12], mizoribine [13] and rituximab [14] for the management of relapse or maintenance of remission. Although in our case series, the relapse in two patients involved the lacrimal glands (Table 5), a recent study by Yamamoto et al. [15] demonstrated that the relapse patterns were not always the same as the clinical form at the first visit. These results highlight the need to monitor not only the first organ but also systemic organs during follow-up of patients with IgG4-RD.

The use of IgG4-specific immunohistochemical staining could help establishing the diagnosis of IgG4-RD in patients with orbital pseudotumor of unknown etiology [6], like Patient 4 in this study. Thus, it is important to perform immunohistochemical staining for IgG4-specific using biopsies from orbital tissues as well as other body organ tissues in order to establish accurate diagnosis and detect any systemic involvement, in patients with suspected IgG4-RD complicated with orbital involvement.

In conclusion, the present study demonstrated that patients with IgG4-RD complicated with orbital involvement often have other organ involvement. The histopathological findings of orbital tissue accorded with characteristic features of IgG4-RD. Lacrimal gland biopsy is a safe procedure compared with that of other tissues such as parotid and submandibular glands, and is a useful diagnostic procedure. Although corticosteroid is effective for orbital involvement and that of other tissues in IgG4-RD, potential relapse should be considered especially during the period of corticosteroid dose tapering.

Acknowledgements

We thank Dr. F. G. Issa for the critical reading of the manuscript.

Authors' contributions

All authors took part in the design of the study, contributed to data collection, participated in writing the manuscript and all agree to accept equal responsibility for the accuracy of the contents of this paper.

Funding

This work was supported in part by Health and Labour Sciences Research Grants for research on intractable diseases (Research on IgG4-RD) from the Ministry of Health, Labour and Welfare of Japan.

Conflict of interest

None.

References

1. Umehara H, Okazaki K, Masaki Y, Kawano M, Yamamoto M, Saeki T, et al. A novel clinical entity, IgG4-related disease (IgG4RD): general concept and details. Mod Rheumatol. 2012;22:1–14.
2. John HS, Yoh Z, Vikram D. IgG4-related disease. N Engl J Med. 2012;366:539–51.
3. Kubota T, Moritani S. Orbital IgG4-related disease: clinical features and diagnosis. ISRN Rheumatol. 2012 (Epub 2012 Jun 21).
4. Go H, Kim JE, Kim YA, Chung HK, Khwarg SI, Kim CW, Jeon YK. Ocular adnexal IgG4-related disease: comparative analysis with mucosa-associated lymphoid tissue lymphoma and other chronic inflammatory conditions. Histopathology 2012;60:296–312.
5. Stone JH, Khosroshahi A, Deshpande V, Chan JK, Heathcote JG, Aalberse R, et al. Recommendations for the nomenclature of IgG4-related disease and its individual organ system manifestations. Arthritis Rheum. 2012;64:3061–7.
6. Wallace ZS, Khosroshahi A, Jakobiec FA, Deshpande V, Hatton MP, Ritter J, et al. IgG4-related systemic disease as a cause of "idiopathic" orbital inflammation, including orbital myositis, and trigeminal nerve involvement. Surv Ophthalmol. 2012;57:26–33.
7. Umehara H, Okazaki K, Masaki Y, Kawano M, Yamamoto M, Saeki T, et al. Comprehensive diagnostic criteria for IgG4-related disease (IgG4-RD), 2011. Mod Rheumatol. 2012;22:21–30.
8. Takahira M, Ozawa Y, Kawano M, Zen Y, Hamaoka S, Yamada K, Sugiyama K. Clinical aspects of IgG4-related orbital inflammation in a case series of ocular adnexal lymphoproliferative disorders. Int J Rheumatol. 2012;2012:635473.
9. Hermet M, André M, Kémény JL, Le Guenno G, Déchelotte P, Guettrot-Imbert G, et al. Is IgG4-related disease a cause of xerostomia? A cohort study of 60 patients. Int J Rheumatol. 2012;2012:303506.
10. Khosroshahi A, Stone JH. Treatment approaches to IgG4-related systemic disease. Curr Opin Rheumatol. 2011;23:67–71.
11. Sandanayake NS, Church NI, Chapman MH, Johnson GJ, Dhar DK, Amin Z, et al. Presentation and management of post-treatment relapse in autoimmune pancreatitis/immunoglobulin G4-associated cholangitis. Clin Gastroenterol Hepatol. 2009;7:1089–96.
12. Naitoh I, Nakazawa T, Ohara H, Sano H, Ando T, Hayashi K, et al. Autoimmune pancreatitis associated with various extrapancreatic lesions during a long-term clinical course successfully treated with azathioprine and corticosteroid maintenance therapy. Intern Med. 2009;48:2003–7.
13. Nanke Y, Kobashigawa T, Yago T, Kamatani N, Kotake S. A case of Mikulicz's disease, IgG4-related plasmacytic syndrome, successfully treated by corticosteroid and mizoribine, followed by mizoribine alone. Intern Med. 2010;49:1449–53.
14. Khosroshahi A, Carruthers MN, Deshpande V, Unizony S, Bloch DB, Stone JH. Rituximab for the treatment of IgG4-related disease: lessons from 10 consecutive patients. Medicine (Baltimore). 2012;91:57–66.
15. Yamamoto M, Takahashi H, Ishigami K, Yajima H, Shimizu Y, Tabeya T, et al. Relapse patterns in IgG4-related disease. Ann Rheum Dis. 2012;71:1755.

Please cite this article in press as: Terao et al., Two Susceptibility Loci to Takayasu Arteritis Reveal a Synergistic Role of the *IL12B* and *HLA-B* Regions in a Japanese Population, The American Journal of Human Genetics (2013), http://dx.doi.org/10.1016/j.ajhg.2013.05.024

ARTICLE

Two Susceptibility Loci to Takayasu Arteritis Reveal a Synergistic Role of the *IL12B* and *HLA-B* Regions in a Japanese Population

Chikashi Terao,[1,2,*] Hajime Yoshifuji,[2] Akinori Kimura,[3] Takayoshi Matsumura,[4] Koichiro Ohmura,[2] Meiko Takahashi,[1] Masakazu Shimizu,[1] Takahisa Kawaguchi,[1] Zhiyong Chen,[3] Taeko K. Naruse,[3] Aiko Sato-Otsubo,[5] Yusuke Ebana,[6] Yasuhiro Maejima,[7] Hideyuki Kinoshita,[8] Kosaku Murakami,[9] Daisuke Kawabata,[2] Yoko Wada,[10] Ichiei Narita,[10] Junichi Tazaki,[11] Yasushi Kawaguchi,[12] Hisashi Yamanaka,[12] Kimiko Yurugi,[13] Yasuo Miura,[13] Taira Maekawa,[13] Seishi Ogawa,[5] Issei Komuro,[4] Ryozo Nagai,[14] Ryo Yamada,[1] Yasuharu Tabara,[1] Mitsuaki Isobe,[7] Tsuneyo Mimori,[2] and Fumihiko Matsuda[1]

Takayasu arteritis (TAK) is an autoimmune systemic vasculitis of unknown etiology. Although previous studies have revealed that HLA-B*52:01 has an effect on TAK susceptibility, no other genetic determinants have been established so far. Here, we performed genome scanning of 167 TAK cases and 663 healthy controls via Illumina Infinium Human Exome BeadChip arrays, followed by a replication study consisting of 212 TAK cases and 1,322 controls. As a result, we found that the *IL12B* region on chromosome 5 (rs6871626, overall $p = 1.7 \times 10^{-13}$, OR = 1.75, 95% CI 1.42–2.16) and the *MLX* region on chromosome 17 (rs665268, overall $p = 5.2 \times 10^{-7}$, OR = 1.50, 95% CI 1.28–1.76) as well as the *HLA-B* region (rs9263739, a proxy of HLA-B*52:01, overall $p = 2.8 \times 10^{-21}$, OR = 2.44, 95% CI 2.03–2.93) exhibited significant associations. A significant synergistic effect of rs6871626 and rs9263739 was found with a relative excess risk of 3.45, attributable proportion of 0.58, and synergy index of 3.24 ($p \leq 0.00028$) in addition to a suggestive synergistic effect between rs665268 and rs926379 ($p \leq 0.027$). We also found that rs6871626 showed a significant association with clinical manifestations of TAK, including increased risk and severity of aortic regurgitation, a representative severe complication of TAK. Detection of these susceptibility loci will provide new insights to the basic mechanisms of TAK pathogenesis. Our findings indicate that *IL12B* plays a fundamental role on the pathophysiology of TAK in combination with HLA-B*52:01 and that common autoimmune mechanisms underlie the pathology of TAK and other autoimmune disorders such as psoriasis and inflammatory bowel diseases in which *IL12B* is involved as a genetic predisposing factor.

Introduction

Takayasu arteritis (TAK [MIM 207600]) is an autoimmune systemic vasculitis that was first reported from Japan.[1] It is estimated that TAK affects around 0.004% of the population in Japan, especially young women aged between 15 and 35. Although TAK was originally thought to affect individuals of mainly Asian origin, individuals with TAK have been identified worldwide, though with lower prevalence compared to Asia.[2] TAK is characterized by the involvement of large arteries, especially the aorta and its large branches, and is grouped into "vasculitis affecting large vessels" according to the Chapel Hill classification.[3] Individuals with TAK develop a wide range of symptoms such as fatigue, syncope, and lowering of vision in addition to its characteristic complications including aortic regurgitation (AR), pulselessness, and difference of blood pressure between right and left upper limbs. Previous studies have revealed that genetic components are involved in the pathogenesis of TAK, and HLA-B*52:01 is so far the only established genetic factor across the world.[4–7] Other genetic components especially outside of the HLA locus have not been confirmed to date. Establishment of association with non-HLA regions would lead to a deeper understanding of the basics of TAK pathology and the development of a novel therapy for this vasculitis. Here, we performed a genome-scanning study of TAK to identify the genetic predisposing factors for TAK.

Subjects and Methods

Study Subjects

A total of 379 TAK cases and 1,985 controls were enrolled in this study. All the cases were diagnosed based on the criteria of

[1]Center for Genomic Medicine, Kyoto University Graduate School of Medicine, Kyoto 606-8507, Japan; [2]Department of Rheumatology and Clinical Immunology, Kyoto University Graduate School of Medicine, Kyoto 606-8507, Japan; [3]Department of Molecular Pathogenesis, Medical Research Institute, Tokyo Medical and Dental University, Tokyo 113-8510, Japan; [4]Department of Cardiovascular Medicine, Graduate School of Medicine, The University of Tokyo, Tokyo 113-8655, Japan; [5]Cancer Genomics Project, Graduate School of Medicine, The University of Tokyo, Tokyo 113-8655, Japan; [6]Department of Bioinformational Pharmacology, Medical Research Institute, Tokyo Medical and Dental University, Tokyo 113-8510, Japan; [7]Department of Cardiovascular Medicine, Tokyo Medical and Dental University, Tokyo 113-8510, Japan; [8]Department of Medicine and Clinical Science, Kyoto University Graduate School of Medicine, Kyoto 606-8507, Japan; [9]Osaka Red Cross Hospital, Osaka 543-8555, Japan; [10]Division of Clinical Nephrology and Rheumatology, Niigata University Graduate School of Medical and Dental Sciences, Niigata 951-8510, Japan; [11]Department of Cardiovascular Medicine, Kyoto University Graduate School of Medicine, Kyoto 606-8507, Japan; [12]Institute of Rheumatology, Tokyo Women's Medical University, Tokyo 162-0054, Japan; [13]Department of Transfusion Medicine and Cell Therapy, Kyoto University Hospital, Kyoto 606-8507, Japan; [14]Jichi Medical University, Tochigi 329-0498, Japan
*Correspondence: a0001101@kuhp.kyoto-u.ac.jp
http://dx.doi.org/10.1016/j.ajhg.2013.05.024.

Please cite this article in press as: Terao et al., Two Susceptibility Loci to Takayasu Arteritis Reveal a Synergistic Role of the *IL12B* and *HLA-B* Regions in a Japanese Population, The American Journal of Human Genetics (2013), http://dx.doi.org/10.1016/j.ajhg.2013.05.024

Table 1. Summary of Study Subjects

	Case	Control
Genome Scanning		
Number	167	663
Age[a]	45.7 ± 15.2	53.5 ± 13.5
Female ratio	0.92	0.74
Age at onset[a]	30.5 ± 14.5	NA
Genotyping	Illumina Infinium Human-Exome BeadChip	Illumina Infinium Human-Exome BeadChip
Subjects with clinical information	AR:87; CRP:89	NA
Institutions	Kyoto University; Tokyo Women's Medical University	Kyoto University
Replication Study		
Number	212	1,322
Age[a]	46.6 ± 17.6	53.3 ± 13.4
Female ratio	0.94	0.62
Age at onset[a]	27.0 ± 11.8	NA
Genotyping	Taqman assay	Illumina Infinium Human Omni 2.5-4 BeadChip, Illumina Infinium Human Omni 2.5-8 BeadChip
Subjects with clinical information	AR:102; CRP:None	NA
Institutions	Tokyo Medical and Dental University; Kyoto University; Niigata University	Kyoto University

Abbreviations are as follows: NA, not applicable; AR, aortic regurgitation; CRP, C-reactive protein.
[a]Mean ± standard deviation (SD).

American College of Rheumatology[8] or guideline provided by Japanese Circulation Society.[9] The control subjects were collected as a part of the Nagahama Prospective Genome Cohort for Comprehensive Human Bioscience (The Nagahama Study), a community-based prospective multiomics cohort study conducted by Kyoto University.[10] This study was approved by the local ethical committees at each institution, and written informed consent was obtained from each subject involved in the study.

Genome Scanning

Illumina Infinium Human Exome BeadChip arrays (Illumina) were used for genome scanning of the cases and the controls. The genome scanning was conducted in Center for Genomic Medicine, Kyoto University Graduate School of Medicine.

Quality Control of Genome Scanning

Polymorphisms showing success rates less than 0.95 in either cases or controls, departure from Hardy-Weinberg equilibrium (HWE) ($p < 1.0 \times 10^{-5}$), or minor allele frequencies less than 0.05 in both cases and controls were excluded from the analysis. Subjects who showed success rates less than 0.95 or evidence of relatedness with other subjects were also excluded. Kinship between study subjects were estimated by PLINK.[11] Quantile-quantile plot (QQ plot) was used to assess the population stratification of the study. Because 1,827 markers over 24,487 were located in the HLA locus in which polymorphisms are very closely linked with each other, the 22,660 markers in the non-HLA regions were used for QQ plot.

Replication Study

The SNPs with p values less than 1.0×10^{-5} in the genome scanning were selected for the replication study. Because the association found in the *HLA-B* region (MIM 142830) was largely attributable to HLA-B*52:01, rs9263739, a proxy of HLA-B*52:01, was selected as a representative of the HLA locus. In the replication study, case samples were genotyped by Taqman Assay (Applied Biosystems) and control genotypes were extracted from array data (Table 1).

Combined Study and Association Study for Genotypes

Association studies of genotypes were performed by chi-square test based on 2 × 2 contingency tables. Combined study of the two studies was performed by inverse-variance method, assuming a fixed-effects model from the effect size (logarithm of odds ratio [OR]) in each study. A significant level for detecting susceptibility genes was set as 2.0×10^{-6}, which was obtained by Bonferroni's correction. A stringent cut-off level of 5.0×10^{-8} was also applied to assess overall significance.

Imputation of Genotypes

Mach dat2 software[12] was used for imputation of the whole genomes based on the results of genome scans with the use of the East Asian panel of HapMap phase II data as reference. SNPs with low imputation scores (Rsq < 0.3) were excluded from the analysis.

Calculation of Linkage Disequilibrium

LD between SNPs in the Illumina Infinium Human Exome BeadChip was assessed based on the genome-scanning data. HapMap project phase II data was used when SNPs were not contained in the array. LD between HLA-B*52:01 and SNPs was calculated by combining our previous HLA-genotyping data of the 173 TAK cases (C.T., unpublished data) by WAKFlow system (Wakunaga Pharmaceutical) with the genome-scanning data.

Estimation of Interaction

We used the method for evaluation of interaction proposed by Andersson et al.[13] Gene-gene interaction was defined as departure from additivity of two loci and measured by three indices based on calculation of relative risk (RR); relative excess risk due to interaction (RERI), attributable proportion (AP), and synergy index (SI). We considered an interaction as significant only when both RERI and AP were different from 0 and additionally SI was more than 1. The very low prevalence of TAK justifies to approximate OR by RR. For instance, when we assessed the interaction between rs9263739 and rs6871626 through these three indices, the subjects were classified into four groups: negative for both rs9263739 T allele and rs6871626 A allele, positive for rs9263739 T allele and negative for rs6871626 A allele, negative for rs9263739 T allele and positive for rs6871626 A allele, and positive for both rs9263739 T allele and rs6871626 A allele. Logistic models were used to calculate the indices.

In Silico Analysis of Association between the Gene Expression and rs6871626

We used two methods to assess the effect of rs6871626 on the *IL12B* (MIM 161561) expression. Gene expression data for *IL12B*